JVI Accepts, published online ahead of print on 14 May 2008
J. Virol. doi:10.1128/JVI.00619-08



# The Immune Response to Herpes Simplex Virus Type 1 Infection in Susceptible Mice is a Major Cause of CNS Pathology Resulting in Fatal Encephalitis.

**Patric Lundberg[1,2†], Chandran Ramakrishna[1], Jeffrey Brown[4], J. Michael Tyszka[5], Mark Hamamura[6], David R. Hinton[7], Susan Kovats[8], Orhan Nalcioglu[6], Kenneth Weinberg[4], Harry Openshaw[3] and Edouard M. Cantin[1,2,3,*].**

*Division of Virology[1], Immunology[2] and Neurology[3], Beckman Research Institute and City of Hope National Medical Center, Duarte, California 91010, USA; Department of Pediatrics, Children's Hospital Los Angele[4]; Los Angeles, California 90033, USA; Division of Biology[5], California Institute of Technology, Pasadena, CA 91125, USA; Center for Functional Onco-Imaging[6], University of California, Irvine, CA 92697, USA; Department of Pathology[7], Keck School of Medicine, Beckman Macular Research Center, University of Southern California, Los Angeles, California 90033, USA; Arthritis & Immunology Research Program[8], Oklahoma Medical Research Foundation, Oklahoma City, OK 73104, USA.*

[*]Corresponding Author: Edouard M. Cantin, Ph.D.
Beckman Research Institute
City of Hope National Medical Center
1500 E. Duarte Road
Duarte, CA 91010, USA
Phone: (626) 301 8480
Fax: (626) 301 8457
Email: ecantin@coh.org

**Running Title:** *Immune pathology in herpes simplex encephalitis*

[†] Present Address: Department of Microbiology
Eastern Virginia Medical School
Norfolk, Virginia
Phone: (757) 446-5174
Fax: (757) 446-7426
Email: lundbeps@evms.edu

**Abstract.**

This study was undertaken to investigate possible immune mechanisms in fatal HSV-1 encephalitis (HSE) after HSV-1 corneal inoculation. Susceptible 129S6 (129) but not resistant C57BL/6 (B6) mice developed intense focal inflammatory brainstem lesions of primarily F4/80$^{+}$ macrophages and Gr-1$^{+}$ neutrophils detectable by MRI as early as day 6 post infection (PI). Depletion of macrophages and neutrophils significantly enhanced survival of infected 129 mice. Immunodeficient B6 (IL-7R$^{-/-}$Kit$^{w41/w41}$) mice lacking adaptive cells (B6-E mice) transplanted with 129 bone marrow showed significantly accelerated fatal HSE compared to B6-E mice transplanted with B6 marrow or control non-transplanted B6-E mice. In contrast, there was no difference in ocular viral shedding in B6-E mice transplanted with 129 bone marrow or B6 bone marrow. Acyclovir treatment of 129 mice beginning day 4 PI (24 h after HSV-1 first reaches the brain stem) reduced nervous system viral titers to undetectable levels but did not alter brainstem inflammation or mortality. We conclude that fatal HSE in 129 mice results from widespread damage in the brainstem caused by destructive inflammatory responses initiated early in infection by massive infiltration of innate cells.

**Introduction.**

Herpes simplex virus type 1 (HSV-1) infections are widespread in developed countries with estimates of seropositivity exceeding 50% (54). Primary infections in immunocompetent individuals are usually mild or even asymptomatic and result in life-long latent infections in sensory ganglia and the central nervous system (CNS) (5). Reactivated HSV-1 can result in recurrent disease of mucous membranes (e.g. gingivostomatitis and herpes labialis) and herpes keratitis, an immunopathological disease that is a leading cause of blindness (39). Also, HSV-1 is the most common cause of fatal, sporadic encephalitis in immunocompetent individuals (40, 56). Improvements in diagnosis and antiviral drug treatment have dramatically reduced morbidity and mortality of HSV-1 encephalitis (HSE) (55), although some patients fail to respond or subsequently suffer neurological relapses after completing a standard treatment course (18, 55).

Clinical and animal model studies have clearly demonstrated the importance of genetic makeup in resistance to a broad range of infectious agents (15, 41). In regard to HSV-1, C57BL/6 (B6) and related B10 mouse strains are resistant, while other strains such A/J, BALB/c, 129S6 (129) and DBA/2J are susceptible to fatal infections (21, 23, 25). In these animal models, mortality results from CNS infection. In prior studies, we defined the herpes resistance locus (*Hrl*) on mouse chromosome 6 (c6) as a major determinant of resistance (22, 25); however, ongoing studies indicate that resistance to HSE is genetically very complex, involving multiple interacting loci with TNF playing a critical role (26) (and manuscript in preparation).

The mechanism by which HSV-1 CNS infection causes death has not been defined. Counter-intuitively, necropsy virus titers of nervous system tissues do not correlate with mouse resistance or susceptibility genotype (25, 26). These and other observations have lead to the suggestion that variation of the host inflammatory response may play a major role determining HSV fatality. Intense inflammatory responses in CNS tissues have been reported in a mouse model of HSE with TNF and macrophage

chemoattractant protein 1 being expressed prominently (43). Also, in vitro and in vivo studies have shown that human and mouse microglia non-productively infected with HSV-1 express a variety of proinflammatory cytokines and chemokines, consistent with their involvement in early innate responses against invading virus (19, 20). Whether such innate inflammatory responses are protective or deleterious has not yet been clarified.

We present here a series of studies comparing HSE in susceptible 129 mice and resistant B6 mice. These studies support the hypothesis that the immune response is the major cause of CNS pathology resulting in a fatal course and that hyper-inflammatory responses initiated by early infiltrating innate cells play a key role in the development of this pathology. Our results have important implications for understanding the pathogenesis and clinical treatment of HSE.

**Materials and Methods.**

**Mouse Strains, HSV Infection and Monitoring.**

The B6-empty strain (B6-E, *IL-7R*$^{-/-}$*,Kit*$^{w41/w41}$) was derived by back crossing the B6.IL-7R$^{-/-}$ strain (B6.129S7-Il7$^{rtm1Imx}$/J) to the B6.Kit$^{w41/w41}$ mutant strain (C57BL/6J-Kit$^{W-41J}$); mice homozygous for both mutations were selected at N10. Both parental strains were obtained from the Jackson Laboratories (Bar Harbor, Maine) as were C57BL/6J mice. 129S6 mice were obtained from Taconic (Germantown, NY) or bred in house. Mice used in experiments were 6 - 10 weeks of age or older (for bone marrow transplantation (BMT) studies). Master stocks of HSV-1 strain 17$^{+}$ comprised of only of cell-released virus were prepared in and titered on mycoplasma-free CV-1 cell monolayers. Single use aliquots of virus in Hanks balanced salt solution (HBSS) supplemented with 2% FBS were stored at –80$^{o}$C. Mice were inoculated as previously described with HSV by corneal scarification with 3.2 x $10^3$ PFU HSV-1 17+, which is 10x $LD_{50}$ for 129S6 mice (25). HSV replication was monitored as shedding of HSV-1 in the tear film as previously described (25). Acyclovir (ACV) 50mg/kg (or PBS control) was administered by intra-

peritoneal injection. The City of Hope Institutional Animal Care and Use Committee approved of all animal procedures that additionally were in compliance with the *Guide for the Care and Use of Laboratory Animals*.

**Isolation of Mononuclear Cells from Brainstems of HSV-1 Infected Mice.**

We adapted the method described by Ford et al (8). Briefly, 2 – 3 pooled brainstems (BS) were minced and digested with collagenase after which the cell suspension was centrifuged through a two-step Percoll gradient. The resulting enriched population of viable mononuclear cells included lymphocytes as well as microglia identified as $CD45^{Int}$ $CD11b^{+}$ $F4/80^{+}$ and CNS macrophages characterized as $CD45^{Hi}$ $CD11b^{+}$ $F4/80^{+}$; these latter two populations are morphologically and functionally distinct (8, 14). Cells isolated using this procedure retained high viability even after further purification by cell sorting provided GKN/BSA buffer was used (8). Mononuclear cell yields from a normal brain range from $0.8 \times 10^5$ to $2 \times 10^5$ with no T cells present (14), but higher cell yields are found for inflamed trigeminal ganglia and brainstem of HSV inoculated mice. Cell viability is usually greater than 95%; control digestions of spleen and draining lymph node (dLN) cells with collagenase indicated that the enzyme had no effect on the expression of cell surface markers or functionality of $CD4^{+}$ and $CD8^{+}$ T cells (33).

**Flow Cytometry.**

Analysis of surface marker expression was done by staining splenocytes or mononuclear cells isolated from the BS of HSV-1 infected mice with fluorochrome-conjugated antibodies. Spleens were mechanically disrupted using sterile glass slides and erythrocytes were lysed using hypotonic buffer. Conventional sandwich ELISA was used to determine the presence of cytokines. A list of antibodies used is provided in **A. Materials and Methods**.

**MRI on live HSV-1 Infected Mice.**

MRI was performed at the Biological Imaging Resource Center at the California Institute of Technology (Caltech) or at the Center for Functional Onco-Imaging, University of California Irvine. Parameters for MR imaging are provided in **A. Material and Methods**.

**In Vivo Depletion of Neutrophils and Macrophages.**

To deplete neutrophils, mice were treated with protein-G purified anti-Gr-1 mAb (RB6-8C5) that binds Ly-6G/C, present on neutrophils (7). The RB6-8C5 hybridoma was provided by Dr. Daniel Berg (University of Iowa) with the permission of Dr. Robert Coffman (formerly of DNAX) (11), and mAb purified from culture supernatants using Protein G columns (HiTrap, Amersham Pharmacia). Each mouse was given 500 μg Gr-1 mAb or rat isotype control antibody by IP injection on day –1, 0, 2, 4, 6 and 8 PI. Neutrophils have been characterized as $CD11b^{+}$, $Ly\text{-}6G^{hi}$ (57), hence their depletion was monitored by staining spleen cells from two mice sacrificed on day 8 PI with antibodies to CD11b and Ly-6G; these mice were not given anti-Ly-6G/C mAb on day 8 PI. **(A. Figure 1A, B)**. Procedures and analysis of Gr-1 mAb cross reactivity are provided in A. **Supplemental Material and Methods**.

Macrophages were depleted in vivo by treating mice with liposome encapsulated dichloromethylene biphosphonate (clodronate) on day 0, 2, 4, 6 and 8 post infection (PI); each mouse received 200 μl clodronate by intraperitoneal (IP) injection. Mice were inoculated with HSV-1 on day 0 and immediately injected with clodronate. Control mice were injected with PBS alone as recommended by the supplier (51). The extent of macrophage depletion was monitored by flow cytometery of pooled peritoneal exudate cells (PECs) stained for CD11b and F4/80. PECs were obtained from two mice

sacrificed on day 8 PI that last received clodronate on day 6; **A. Figure 1 M and N** shows > 95% depletion of $CD11b^+$ cells in this analysis.

**Histology and Immunostaining.**

Anesthetized mice were sacrificed by cardiac perfusion of PBS at room temperature. Brainstems were either (i) snap frozen in liquid nitrogen cooled isopentane, embedded in O.C.T., and cut in 6 um sections or (ii) perfused with cold 4% paraformaldehyde, incubated overnight in 4% paraformaldehyde, embedded in paraffin, and cut in 100 μm step sections with multiple 6 um serial sections collected at each step. For paraffin sections, the first section from each step was stained with hematoxylin and eosin (H&E) and serial adjacent sections from the most affected steps were stained for the presence of $Gr\text{-}1^+$ neutrophils, $F4/80^+$ macrophages (mAb clone A3-1), $CD4^+$ (mAb clone GK1.5) and $CD8^+$ (mAb clone 53-6.72) T cells, and HSV antigen (rabbit polyclonal DAKO, Glostrup, Denmark) using standard immunohistochemistry (Vector ABC Elite, AEC chromogen). Spleen sections were used as positive controls and primary antibodies were omitted for negative controls.

**Bone Marrow Transplantation.**

B6-E mice (B6.IL-$7R^{-/-}$ $Kit^{w41/w41}$) were used as recipients for bone marrow transplantation (BMT). The dominant negative $Kit^{w41/w41}$ mutation affects primarily the kinase but not other aspects of the c-Kit receptor (34). The B6-E mouse lacks αβ T, mature B ($CD19^+$ early pro-B cells are present as expected (10, 53) (***S. Figure 2A***) and γδ T cells as a result of IL-7R deficiency and the $Kit^{w41/w41}$ mutation (9, 13, 31, 37) but monocyte subsets, NK cells (***S. Figure 2A)*** and DCs (***S. Figure 2B and C)*** were present at levels comparable to B6. Kit mutations additionally interfere with mast cell (MC) development and function, and B6-E mice like $Kit^{W/W\text{-}v}$ mice, are deficient in tissue mast cells (17, 28, 38).

Six week old B6-E mice, either irradiated with 650 rads or non-irradiated, were reconstituted with 129 or B6 bone marrow. Retro-orbital bleeds at about 10 weeks post transplantation were analyzed for B (CD19) and T (Thy1.2) cells to validate engraftment (not shown). In irradiated mice roughly 70% of the macrophages and all of the B and T cells are donor derived. At about12 weeks the different mouse groups were blind challenged with HSV-1. Although, B6 and 129 mice are histocompatible they do differ at minor MHC loci, hence, it was important to exclude the possibility of development of GVHD for cross strain bone marrow transplants. Examination of liver and small intestine tissue H&E sections obtained from 4 – 5 normally engrafted mice in each transplant group failed to reveal morphologic changes typical of GVHD (not shown); the pathology report stated all tissue sections appeared morphologically normal, which excludes GVHD as a confounding factor in the transplant experiments.

**Statistical Analysis**

Mortality data was analyzed by Log-rank testing (takes into account both time of death and final mortality). Titers and cytokine production (averages ± SEM) was analyzed using two-tailed Student's T-test or Mann-Whitney test where appropriate, and judged significant if $p<0.05$. Flow cytometry data was judged to be different based on mean channel changes of replicate test versus control samples or greater than 2-fold changes in relative or absolute numbers of cells as appropriately applicable.

**Results.**

**Visualization of Brainstem Inflammation by MRI and Immunohistopathology in Susceptible 129 and Resistant B6 Mice**

To compare brain stem (BS) infection, B6 or 129 mice were inoculated with HSV by corneal scarification and representative mice were anesthetized for MRI scan at day 6 PI. Increased signals on T2-weighted sequences were seen corresponding to the trigeminal root entry zone and nuclei in 129 but not in B6 mice (**Figure 1A & B**). To confirm that this increased signal (reflecting focal edema indicated by the arrow in **Figure 1A** was secondary to inflammation, cryosections were prepared from 129 and B6 mice on day 7 PI for H&E and immunostaining. BS sections from 129 animals showed multifocal areas of meningoencephalitis, consistent with the MRI. In some areas the inflammatory infiltrate was associated with fibrinoid vasculitis (not shown) and necrosis of associated brain stem parenchyma (**Figure 1, C-D**). On H&E sections, the infiltrate was mixed (**C**), however neutrophils appeared to predominate. The inset shows the infiltrate at higher magnification and the black arrow points to cells with neutrophil morphology while the white arrow points to a mononuclear cell. In contrast, brainstem sections from B6 animals were for the most part normal with only rare inflammatory cells within the subarachnoid space or parenchyma, and no areas of necrosis (**D**). Immunohistochemical staining of 129 sections showed extensive infiltration of the tissue with macrophages (**E)** and neutrophils **(G**, arrows point to immunoreactive cells with neutrophil morphology). Scattered $CD4^+$ and $CD8^+$ cells were seen infiltrating intact tissues adjacent to more inflamed necrotic regions (**I & K**). Staining for HSV antigens revealed numerous immunoreactive cells (**M**), including neurons (indicated by the arrow) but the antigen positive cells did not appear localized to areas of inflammation. Macrophages were absent in B6 BS sections (**F**) except for focal areas in which a mild increase in macrophages was seen in the subarachnoid space (not shown). There were no neutrophils or $CD8^+$ T cell infiltrates (**H & L**); however occasional perivascular $CD4^+$ cells were noted (**J**). HSV antigen staining was negative (**N**). Remarkably, HSV-1 was cleared from the BS of wild type B6 mice in the virtual absence of inflammatory responses detectable either by MRI or histology at day 6 - 7 PI. In contrast, the massive tissue destruction observed in the BS of 129 mice was associated with a dramatic influx of predominantly neutrophils and macrophages and the persistence of HSV-1 antigen.

**Analysis of Isolated Brainstem Immune Cells Early in HSV-1 Infection of Susceptible 129 and Resistant B6 Mice.**

To further determine differences in inflammatory responses in B6 and 129 mice, infiltrating brain stem (BS) CD45+ mononuclear cells were analyzed by flow cytometry. Macrophages comprised over 75% of infiltrating cells in both strains at day 6 PI, and there was about a 4-fold increase in the macrophage compartment in both strains by day 12 PI. As shown in **Figure 2A**, there were 9-10 fold more macrophages present in 129 mice at both days 6 and 12 PI. Activated macrophages, as indicated by MHC class II expression (closed bars in **Figure 2A**) were 58-fold greater in 129 mice at day 6 and 24-fold greater at day 12 PI (**Figure 2C**). Although more microglial cells were isolated from B6 brainstem (Figure 2B), 129 microglia expressed 13.7 higher levels of MHC II at day 6 PI, as indicated by MHC II density (**Figure 2C**) reflecting a more activated state. Only a few $CD4^+$ and $CD8^+$ T cells were present in 129 BS at day 6 PI while T cells were not present in B6 BS. By day 12 PI, T cells were seen in the BS of both mouse strains however their numbers were 3-4 fold greater in 129 BS (**Figure 2E**). These differences in T cell accumulation and MHC II expression in the BS reflects the overall greater inflammatory response in 129 compared to B6 mice.

To investigate whether the microglial activation in 129 CNS extended beyond the BS, cells were isolated from whole brain and spinal cord on day 12 PI and analyzed by flow cytometry for MHC II expression. **Figure 2D** shows significantly higher activation of $CD45^{int}$ $F4/80^+$ microglia in all three CNS compartments in 129 compared to B6 mice as judged by MHC II expression. Differences in MHC II expression were most pronounced in brain and spinal cord. Greater than 97% of microglia were MHC $II^+$ with an MFI (mean florescent intensity) above 1200 in 129 mice, while fewer than 30% of B6 microglia were MHC $II^+$ with an MFI less than 100 (**Figure 2D**).

Next we focused on early innate responses in 129 mice to identify the cell types underlying development of inflammatory lesions in the BS. From 38 h through day 9 PI the number of activated $CD11b^+$ $F4/80^+$ monocytes expressing MHC class II increased steadily (**Figure 3A** and **3E**). Separation of the $CD11b^+$ $F4/80^+$ population based on CD45 expression revealed that increased MHC class II expression was due primarily to activation of microglia ($CD11b^+$ $F4/80^+$ $CD45^{Int}$) and to a lesser extent, macrophages ($CD11b^+$ $F4/80^+$ $CD45^{Hi}$) infiltration (**Figure 3A** and **3E**). Although, as a percentage of total mononuclear cells macrophage numbers did not change markedly, their absolute numbers increased from 62 h through day 9 PI as much as 13-fold (**Figure 3F**, shows change relative to cells from naïve mice below each panel in **Figure 3E**, indicated as microglia, MG, and macrophages, MP). Marked activation of microglia occurred between day 4 and day 7 PI (50-fold) and was sustained through day 9 (100-fold) as evidenced by up-regulation of MHC class II expression (**Figure 3E**).

Mononuclear cells infiltrating the BS of mock or HSV-1 infected mice at day 7 PI were stained for CD4 or CD8 and CD62L to determine their activation status in comparison to $CD4^+$ and $CD8^+$ T cells isolated from the dLN. As expected, there were significantly more cells in the dLN of infected compared to mock infected mice, $5 \times 10^7$ and $1.75 \times 10^6$ cells per mouse, respectively. Activated $CD4^+$ and $CD8^+$ T cells displaying a highly activated phenotype ($CD62L^{low}$) were 4-5 fold more numerous in infected than uninfected dLN (**Figure 3C**). Although, approximately twice as many mononuclear cells infiltrated the BS of infected compared to mock infected mice at day 7 PI ($1.85 \times 10^5$ events per infected BS compared to $1.02 \times 10^5$ events per mock infected BS), $CD4^+$ and $CD8^+$ T cells were largely absent (**Figure 3D**). However, by day 13 PI the BS contained significant numbers of activated $CD4^+$ and $CD8^+$ T cells (18.0% and 14.9%, respectively of the infiltrating mononuclear cell population; not shown). Thus, although activated T cells are plentiful in the dLN at day 7 PI their accumulation in the infected BS is delayed until after day 8 PI as we previously reported (4).

Differences in cellular CNS infiltration between 129 and B6 mice during acute infection could relate to differences in sensing HSV-1 infection. We examined expression of selected TLRs on peritoneal exudate (PE) macrophages because in vivo depletion during infection confirmed their involvement in pathogenesis of HSE (26). As determined by real time PCR, expression of TLR9 was 2.2 fold higher in 129 than B6 macrophages (**Table 1**. Although, TLR2, 4 and 7 were expressed at equivalent levels), TLR6 which is known to cooperate with TLR2 for recognition of lipopeptides was expressed at markedly increased levels on 129 (480 fold higher) compared to B6 PE macrophages (**Table 1**).

**Depletion of Neutrophils or Macrophages During HSV-1 Infection Increases Survival of 129 Mice.**

To determine the protective effect of neutrophils and macrophages on mortality, cell depletion studies were done administering anti-Gr-1 mAb or clodronate respectively to HSV-1 inoculated 129 mice. As shown in **Figure 4,** median survival was 4-5 days longer in depleted mice (p= 0.007 for neutrophil depletion and p = 0.012 for macrophage depletion). 129 mice depleted of both neutrophils and macrophages did not show any additional survival advantage, and by day 11 there was no difference in mortality in any of the treatment groups compared to mock-treated controls probably due to the rapid reappearance of neutrophils as noted in earlier studies (1, 46, 48) and shown here by the tendency for rapid reappearance of Gr-$1^+$ cells (**Appendix (A) Figure 1A & B**). The timing of repopulation of the spleen by different macrophage subsets is variable after clodronate treatment (6, 32).

**Transfer of Resistance or Susceptibility to Fatal HSE by Bone Marrow Transplantation (BMT): Effect on Brain Stem MRI, Histopathology, and HSV-1 Tear Film Shedding.**

Prolongation of survival by cell depletion in susceptible 129 mice (**Figure 4**) suggests the possibility that mouse strain differences in resistance to HSE may at least in part be encoded in hematopoietic cells. To investigate this possibility, we transplanted bone marrow from H-$2^b$ MHC

histocompatible donor 129 or B6 mice into immunodeficient B6 empty recipient mice (B6-E) that were gamma-irradiated or non-irradiated. Regardless of irradiation status, all B6-E mice receiving B6 bone marrow transplants survived (and these 2 groups are combined in **Figure 5**). In contrast, there was significant mortality with 129 bone marrow transplants in both non-irradiated B6-E recipients ($p< 0.05$ compared to B-6 marrow transplants) and B6-E recipients that were γ-irradiated to ablate endogenous innate immune cells ($p < 0.01$ compared to B6 marrow transplants). Although survival was lower for the irradiated compared to the non-irradiated group receiving 129 bone marrow (9/16 survival, 56% versus 10/13 survival, 77%), given the number of mice used this difference in mortality did not reach statistical significance. Overall survival was 50% (13/26) in control, infected B6-E mice not given bone marrow transplant. This survival was statistically worse than for the non-irradiated 129 bone marrow transplant group ($p<0.05$) but not the radiated group, a finding that is consistent with B6-derived innate immune responses being protective. More persuasive of a protective effect of B6 innate cells is early death and poor overall survival (less than 20%) of wild type 129 mice: more than twice the mortality of B6-E mice, with or without marrow transplant. As further shown in **Figure 5A**, mortality in the control, non-transplanted B6-E mice was delayed relative to the 129 bone marrow transplant recipients, beginning at day 15 PI. From days 17 through 21 PI (marked by horizontal arrow in **Figure 5A**), cumulative mortality was significantly greater in the 129 bone marrow transplanted compared to non-transplanted control B6-E mice ($p=0.008$ to 0.026). These results indicate that 129 hematopoietic cells transfer HSE susceptibility resulting in accelerated mortality compared to control non-transplanted B6-E mice lacking adaptive immunity.

To determine if the degree of brain stem inflammation correlated with these mortality results, MRI scans on day 6 PI and histopathology studies on day 7 PI were carried out in transplanted mice. As anticipated, B6-E mice transplanted with 129 marrow had an increased signals on T2 MRI corresponding to the trigeminal root entry zone, similar to what is shown in **Figure 1A**; whereas, no MRI lesions were detected in B6-E mice transplanted with B6 marrow (not shown). Similarly, B6-E mice transplanted with

129 but not B6 bone marrow had leptomeningeal focal inflammatory cell infiltrates and multiple perivascular and subpial lesions with prominent neutrophils and macrophages (**Figure 5 C, D, E, F**). The pathology was most prominent in irradiated B6-E mice transplanted with 129 bone marrow. Only occasional viral inclusion bodies were noted in non-transplanted B6-E mice; whereas very prominent inclusion bodies in trigeminal neuronal nuclei were seen in B6-E mice transplanted with 129 bone marrow, especially irradiated 129 bone marrow (not shown).

To determine whether the differences in mortality and inflammation in transplanted B6-E mice are also reflected in differences of HSV replication, eye swab cultures were obtained daily after HSV inoculation by the corneal route. As shown in **Figure 5B**, there was no significant difference in duration of HSV shedding in B6-E mice transplanted with either B6 or 129 bone marrow (either irradiated or non-irradiated). In contrast, non-transplanted B6-E mice shed virus for 14 days, 1 week longer then any of the transplant groups. This result is analogous to our prior study showing equivalent necropsy HSV titers in trigeminal ganglia and brainstem of susceptible 129 and resistant B6 mice; i.e., HSV titers are not predictive of strain-specific mortality (25).

**Acyclovir (ACV) Treatment Controls HSV Replication But Does Not Prevent Brain Stem Inflammation and Mortality in 129 Mice.**

To support the hypothesis that HSE mortality in this mouse model may be related to bystander inflammation, an attempt was made to separate the effect of viral cytopathology from brainstem inflammation by ACV treatment of HSV-inoculated 129 mice. Timing of treatment was critical in these trials. Virus has been shown to reach the brain stem by day 3 after corneal inoculation of HSV (44). When ACV treatment was started on day 2 PI, brainstem infection, mortality, and brainstem inflammation were all blocked (not shown). However as shown in **Figure 6A**, ACV initiated on day 4 PI reduced viral titers to low or undetectable levels in both trigeminal ganglia and brainstem homogenates assayed on day 6 PI.

Despite absence of ongoing HSV replication, mortality in the ACV treated mice occurred in the usual time course from day 6 to 12 PI (**Figure 6B**). By day 8 PI, infectious HSV was no longer detectable in brainstem of sacrificed control and ACV treated mice (**Figure 6A**). Necropsy brainstem homogenates of mice in both groups succumbing to the infection on day 9 PI and later were negative for infectious HSV although virus was present in control mice that died earlier (not shown). Even though ACV suppressed HSV brain stem replication, the brain stem inflammatory infiltrate was equivalent in control and ACV treated mice (**Figure 6C**). These results demonstrate that although HSV invasion is required to initiate brainstem inflammation, the inflammation progresses in the absence of viral replication and mortality correlates with inflammation rather than ongoing viral replication.

**Discussion:**

Our working hypothesis is that tightly regulated innate responses in B6 mice are critical for early restriction of HSV-1 replication. HSV-1 invades the CNS by day 3 PI (44), well before arrival of activated HSV-1 specific T cells, which usually are not detectable until day 8 PI (4). While $CD8^+$ T cells have been shown to be proficient at clearing virus late in infection, they do not play a role in limiting spread of virus from peripheral sites of infection to sensory ganglia and the CNS (16, 50). Neurons themselves might also contribute to restriction of HSV-1 replication in the CNS of B6 mice. Notably, the response of different trigeminal ganglion neurons to HSV-1 infection ranges from permissive to restrictive as assessed by antigen and LAT expression (27). Additionally, in response to IFN-$\alpha$, neurons mount STAT1 dependent responses that reflect the induction of potent innate antiviral mechanisms (52). Consistent with this idea, in a related study we report strong induction of STAT1 expression in trigeminal ganglia of HSV-1 infected 129 mice at day 4 PI (24). Local B6-derived CNS innate immunity may also explain the greater resistance of B6-E mice transplanted with 129 bone marrow compared to wild type 129 mice and also the improved survival of the non-irradiated B6-E mice transplanted with 129 bone marrow compared to the $\gamma$-irradiated transplanted group (**Figure 5**).

Although the innate responses in B6 and 129 mice differ, our hypothesis is that the greater inflammatory response in 129 brainstem (**Figure 1 and 2**) results not so much from greater restriction of viral replication in B6 mice but from failure to modulate inflammatory responses in 129 mice. Support of this conclusion is that brainstem inflammation was equivalent in control PBS-treated 129 mice and mice treated with acyclovir to suppress viral replication (**Figure 6C**). Acyclovir in these trials was begun 4 days PI, just 24h after HSV reaches the brainstem from the corneal site of inoculation (44). We speculate that differences in TLR signaling in HSV infected 129 and B6 mice may result in differences in activation and chemokine signaling in the brain (2, 20), providing a plausible mechanism to account for the vastly different inflammatory responses observed in the brainstem.

A number of observations argue in favor of brainstem inflammation as a major determinant of mortality in this mouse model of HSE. We previously reported increased survival in HSV-inoculated 129 mice treated with monoclonal antibodies to MIG and IP-10 to block CXCR3 signaling; and there was increased survival and decreased brain stem inflammation in CXCR3 genetically depleted BALB/c mice inoculated with HSV (24). In the present report, we show (1) marked brain stem inflammation in HSE susceptible 129 mice compared to resistant B6 mice, (2) enhanced survival in 129 mice depleted of either macrophages or neutrophils, and (3) an accelerated course of fatal HSE in immunodeficient B6 mice given a 129 bone marrow graft. Consistent with an inflammatory bystander mechanism rather than ongoing viral cytopathology, ACV treatment of 129 mice cleared infectious HSV but did not prevent inflammation or mortality in HSV-inoculated 129 mice (**Figure 6**). Prominence of macrophages and neutrophils with a paucity of T cells in the brainstem inflammatory infiltrate supports a bystander mechanism involving innate cells. Oxidative damage as indicated by expression of F4-neuroprostanes and F-2 isoprostanes have been reported in association of neutrophil influx in HSV-infected Balb/c mouse brains (34). This oxidative damage is a likely major mechanism in fatal HSE (30, 49).

The results presented here have important clinical implications for treatment of HSE. Arguments in favor of immune mechanisms in the pathology of fatal HSE have emerged from clinical observations and experimental animal studies (18, 36). HSE occurring during primary infection in neonates may be difficult to diagnose and if not treated promptly is invariably fatal. However, even when diagnosed and treated with high dose ACV for 21 days a substantial number of infants with HSE die (3, 35). Moreover, a 2006 study investigating the incidence and pathogenesis of clinical relapse after HSE in adults lends support to immunological mechanisms rather than direct viral cytotoxicity (45). A recent study of HSE in a mouse model using serial cranial MRI reported a significant reduction in the severity of long-term MRI abnormalities in mice treated with ACV in combination with corticosteroids, but not in mice treated with ACV or PBS alone (29). Importantly, clinical improvement in abnormal MRI findings was independent of virus load as both groups of ACV treated mice showed a dramatic reduction in virus load in the brain (29). Additionally, it has been reported that corticosteroid treatment does not increase HSV-1 replication and dissemination in a rat model of focal encephalitis (47). However, it was recently reported that the timing of treatment with immunosuppressive steroids is critical (42), consistent with a balanced immune response being required for survival. These results demonstrating a beneficial effect of combined ACV and corticosteroid therapy over ACV alone are consistent with host immune responses to HSV-1 being a significant cause of long-term MRI abnormalities in the brain (29, 36, 47). Results from a recent nonrandomized retrospective study using multiple logistic regression analysis identified corticosteroid use as an independent predictor of improved clinical outcome when administered with conventional ACV therapy indicate the utility of studies conducted in the mouse model (12).

Our data suggest that strategies designed to block or reduce macrophage/microglial and/or neutrophil responses in the CNS of some HSE patients may be beneficial and result in improved survival with reduced morbidity. However, caution is warranted in the application of therapies targeting specific innate cell types, as we have demonstrated that macrophages are protective in the resistant B6 background (26). Ideally, a genetic test to identify at risk individuals who are genetically susceptible to HSE would

facilitate implementation of such targeted immunotherapy and this may emerge from our studies of genetic resistance to HSE.

**Acknowledgements:**

We thank Paula V. Welander and Seung-Jae Jung for technical assistance. This research was supported by grants EY013814 and AI060038 from the National Institutes of Health, National Eye Institute and National of Allergy and Infectious Diseases, respectively.

**References:**

1. **Andrews, D. M., V. B. Matthews, L. M. Sammels, A. C. Carrello, and P. C. McMinn.** 1999. The Severity of Murray Valley Encephalitis in Mice Is Linked to Neutrophil Infiltration and Inducible Nitric Oxide Synthase Activity in the Central Nervous System. J. Virol. **73:**8781-8790.
2. **Aravalli, R. N., S. Hu, T. N. Rowen, J. M. Palmquist, and J. R. Lokensgard.** 2005. Cutting Edge: TLR2-Mediated Proinflammatory Cytokine and Chemokine Production by Microglial Cells in Response to Herpes Simplex Virus. J Immunol **175:**4189-4193.
3. **Bale, J. F., and L. J. Miner.** 2005. Herpes Simplex Virus Infections of the Newborn. Curr Treat Options Neurol **7:**151-156.
4. **Cantin, E. M., D. R. Hinton, J. Chen, and H. Openshaw.** 1995. Gamma interferon expression during acute and latent nervous system infection by herpes simplex virus type 1. J. Virol. **69:**4898-4905.

5. **Chen, S.-H., H.-W. Yao, W.-Y. Huang, K.-S. Hsu, H.-Y. Lei, A.-L. Shiau, and S.-H. Chen.** 2006. Efficient Reactivation of Latent Herpes Simplex Virus from Mouse Central Nervous System Tissues. J. Virol. **80:**12387-12392.

6. **Ciavarra, R. P., L. Taylor, A. R. Greene, N. Yousefieh, D. Horeth, N. van Rooijen, C. Steel, B. Gregory, M. Birkenbach, and M. Sekellick.** 2005. Impact of macrophage and dendritic cell subset elimination on antiviral immunity, viral clearance and production of type 1 interferon. Virology **342:**177-189.

7. **Fleming, T. J., M. L. Fleming, and T. R. Malek.** 1993. Selective expression of Ly-6G on myeloid lineage cells in mouse bone marrow. RB6-8C5 mAb to granulocyte-differentiation antigen (Gr-1) detects members of the Ly-6 family. J Immunol **151:**2399-408.

8. **Ford, A. L., A. L. Goodsall, W. F. Hickey, and J. D. Sedgwick.** 1995. Normal adult ramified microglia separated from other central nervous system macrophages by flow cytometric sorting. Phenotypic differences defined and direct ex vivo antigen presentation to myelin basic protein- reactive CD4+ T cells compared. J Immunol **154:**4309-21.

9. **Fry, T. J., and C. L. Mackall.** 2001. Interleukin-7: master regulator of peripheral T-cell homeostasis? Trends in Immunology **22:**564-71.

10. **Hesslein, D. G. T., S. Y. Yang, and D. G. Schatz.** 2006. Origins of peripheral B cells in IL-7 receptor-deficient mice. Molecular Immunology **43:**326-334.

11. **Ismail, H. F., P. Fick, J. Zhang, R. G. Lynch, and D. J. Berg.** 2003. Depletion of Neutrophils in IL-10-/- Mice Delays Clearance of Gastric Helicobacter Infection and Decreases the Th1 Immune Response to Helicobacter. J Immunol **170:**3782-3789.

12. **Kamei, S., T. Sekizawa, H. Shiota, T. Mizutani, Y. Itoyama, T. Takasu, T. Morishima, and K. Hirayanagi.** 2005. Evaluation of combination therapy using aciclovir and corticosteroid in adult patients with herpes simplex virus encephalitis. J Neurol Neurosurg Psychiatry **76:**1544-9.

13. **Kang, J., M. Coles, and D. H. Raulet.** 1999. Defective development of gamma/delta T cells in interleukin 7 receptor-deficient mice is due to impaired expression of T cell receptor gamma genes. The Journal of Experimental Medicine **190:**973-82.

14. **Krakowski, M. L., and T. Owens.** 1997. The central nervous system environment controls effector CD4+ T cell cytokine profile in experimental allergic encephalomyelitis. Eur J Immunol **27:**2840-7.

15. **Kramnik, I., and V. Boyartchuk.** 2002. Immunity to intracellular pathogens as a complex genetic trait. Current Opinion in Microbiology **5:**111-117.

16. **Lang, A., and J. Nikolich-Zugich.** 2005. Development and Migration of Protective CD8+ T Cells into the Nervous System following Ocular Herpes Simplex Virus-1 Infection. J Immunol **174:**2919-2925.

17. **Lantz, C. S., J. Boesiger, C. H. Song, N. Mach, T. Kobayashi, R. C. Mulligan, Y. Nawa, G. Dranoff, and S. J. Galli.** 1998. Role for interleukin-3 in mast-cell and basophil development and in immunity to parasites. Nature **392:**90-3.

18. **Lellouch_Tubiana, A., M. Fohlen, O. Robain, and F. Rozenberg.** 2000. Immunocytochemical characterization of long-term persistent immune activation in human brain after herpes simplex encephalitis. Neuropathology and Applied Neurobiology **26:**285-94.

19. **Lokensgard, J. R., M. C. Cheeran, S. Hu, G. Gekker, and P. K. Peterson.** 2002. Glial cell responses to herpesvirus infections: role in defense and immunopathogenesis. The Journal of Infectious Diseases **186 Suppl 2:**S171-9.

20. **Lokensgard, J. R., S. Hu, W. Sheng, M. vanOijen, D. Cox, M. C. Cheeran, and P. K. Peterson.** 2001. Robust expression of TNF-alpha, IL-1beta, RANTES, and IP-10 by human microglial cells during nonproductive infection with herpes simplex virus. J Neurovirol **7:**208-19.

21. **Lopez, C.** 1975. Genetics of natural resistance to herpesvirus infections in mice. Nature **258:**152-153.

22. **Lopez, C.** 1981. Resistance to herpes simplex virus - type 1 (HSV-1). Curr Top Microbiol Immunol **92:**15-24.

23. **Lopez, C.** 1980. Resistance to HSV-1 in the mouse is governed by two major, independently segregating, non-H-2 loci. Immunogenetics **11:**87-92.

24. **Lundberg, P., H. Openshaw, M. Wang, H. J. Yang, and E. Cantin.** 2007. Effects of CXCR3 Signaling on Development of Fatal Encephalitis and Corneal and Periocular Skin Disease in HSV-Infected Mice Are Mouse-Strain Dependent. Invest Ophthalmol Vis Sci **48:**4162-70.

25. **Lundberg, P., P. Welander, H. Openshaw, C. Nalbandian, C. Edwards, L. Moldawer, and E. Cantin.** 2003. A locus on mouse chromosome 6 that determines resistance to herpes simplex virus also influences reactivation, while an unlinked locus augments resistance of female mice. J Virol **77:**11661-73.

26. **Lundberg, P., P. V. Welander, C. K. Edwards, III, N. van Rooijen, and E. Cantin.** 2007. Tumor Necrosis Factor (TNF) Protects Resistant C57BL/6 Mice against Herpes

Simplex Virus-Induced Encephalitis Independently of Signaling via TNF Receptor 1 or 2. J. Virol. **81:**1451-1460.

27. **Margolis, T. P., F. Sedarati, A. T. Dobson, L. T. Feldman, and J. G. Stevens.** 1992. Pathways of viral gene expression during acute neuronal infection with HSV-1. Virology **189:**150-60.

28. **Metcalfe, D. D., D. Baram, and Y. A. Mekori.** 1997. Mast cells. Physiol Rev **77:**1033-79.

29. **Meyding-Lamade, U. K., C. Oberlinner, P. R. Rau, S. Seyfer, S. Heiland, J. Sellner, B. T. Wildemann, and W. R. Lamade.** 2003. Experimental herpes simplex virus encephalitis: a combination therapy of acyclovir and glucocorticoids reduces long-term magnetic resonance imaging abnormalities. J Neurovirol **9:**118-25.

30. **Milatovic, D., Y. Zhang, S. J. Olson, K. S. Montine, L. J. Roberts, 2nd, J. D. Morrow, T. J. Montine, T. S. Dermody, and T. Valyi-Nagy.** 2002. Herpes simplex virus type 1 encephalitis is associated with elevated levels of F2-isoprostanes and F4-neuroprostanes. J Neurovirol **8:**295-305.

31. **Miller, C. L., V. I. Rebel, C. D. Helgason, P. M. Lansdorp, and C. J. Eaves.** 1997. Impaired steel factor responsiveness differentially affects the detection and long-term maintenance of fetal liver hematopoietic stem cells in vivo. Blood **89:**1214-23.

32. **Naito, M., S. Umeda, T. Yamamoto, H. Moriyama, H. Umezu, G. Hasegawa, H. Usuda, L. D. Shultz, and K. Takahashi.** 1996. Development, differentiation, and phenotypic heterogeneity of murine tissue macrophages. J Leukoc Biol **59:**133-138.

33. **Niemialtowski, M. G., and B. T. Rouse.** 1992. Predominance of Th1 cells in ocular tissues during herpetic stromal keratitis. J Immunol **149:**3035-9.

34. **Nocka, K., J. C. Tan, E. Chiu, T. Y. Chu, P. Ray, P. Traktman, and P. Besmer.** 1990. Molecular bases of dominant negative and loss of function mutations at the murine c-kit/white spotting locus: W37, Wv, W41 and W. Embo J **9:**1805-13.

35. **O'Riordan, D. P., W. C. Golden, and S. W. Aucott.** 2006. Herpes Simplex Virus Infections in Preterm Infants. Pediatrics **118:**e1612-1620.

36. **Openshaw, H., and E. M. Cantin.** 2005. Corticosteroids in herpes simplex virus encephalitis. J Neurol Neurosurg Psychiatry **76:**1469.

37. **Peschon, J. J., P. J. Morrissey, K. H. Grabstein, F. J. Ramsdell, E. Maraskovsky, B. C. Gliniak, L. S. Park, S. F. Ziegler, D. E. Williams, C. B. Ware, and et al.** 1994. Early lymphocyte expansion is severely impaired in interleukin 7 receptor-deficient mice. J Exp Med **180:**1955-60.

38. **Reith, A. D., R. Rottapel, E. Giddens, C. Brady, L. Forrester, and A. Bernstein.** 1990. W mutant mice with mild or severe developmental defects contain distinct point mutations in the kinase domain of the c-kit receptor. Genes Dev **4:**390-400.

39. **Roizman, B., and A. E. Sears.** 1987. An inquiry into the mechanisms of herpes simplex virus latency. Annu. Rev. Microbiol. **41:**543-577.

40. **Roos, K. L.** 1999. Encephalitis. Neurologic clinics **17:**813 (22 pages).

41. **Segal, S., and A. V. Hill.** 2003. Genetic susceptibility to infectious disease. Trends Microbiol **11:**445-8.

42. **Sergerie, Y., G. Boivin, D. Gosselin, and S. Rivest.** 2007. Delayed but Not Early Glucocorticoid Treatment Protects the Host during Experimental Herpes Simplex Virus Encephalitis in Mice. J Infect Dis **195:**817-825.

43. **Sergerie, Y., S. Rivest, and G. Boivin.** 2007. Tumor Necrosis Factor,ÄìŒ± and Interleukin,Äê1Œ≤ Play a Critical Role in the Resistance against Lethal Herpes Simplex Virus Encephalitis. The Journal of Infectious Diseases **196:**853-860.

44. **Shimeld, C., S. Efstathiou, and T. Hill.** 2001. Tracking the Spread of a lacZ-Tagged Herpes Simplex Virus Type 1 between the Eye and the Nervous System of the Mouse: Comparison of Primary and Recurrent Infection. J. Virol. **75:**5252-5262.

45. **Sköldenberg, B., E. Aurelius, A. Hjalmarsson, F. Sabri, M. Forsgren, B. Andersson, A. Linde, S. Ö, M. Studahl, L. Hagberg, and L. Rosengren.** 2006. Incidence and pathogenesis of clinical relapse after herpes simplex encephalitis in adults. Journal of neurology **253:**163-170.

46. **Thomas, J., S. Gangappa, S. Kanangat, and B. T. Rouse.** 1997. On the essential involvement of neutrophils in the immunopathologic disease: herpetic stromal keratitis. J Immunol **158:**1383-91.

47. **Thompson, K. A., W. W. Blessing, and S. L. Wesselingh.** 2000. Herpes simplex replication and dissemination is not increased by corticosteroid treatment in a rat model of focal Herpes encephalitis. Journal of Neurovirology **6:**25-32.

48. **Tumpey, T. M., S. H. Chen, J. E. Oakes, and R. N. Lausch.** 1996. Neutrophil-mediated suppression of virus replication after herpes simplex virus type 1 infection of the murine cornea. J Virol **70:**898-904.

49. **Valyi-Nagy, T., S. J. Olson, K. Valyi-Nagy, T. J. Montine, and T. S. Dermody.** 2000. Herpes Simplex Virus Type 1 Latency in the Murine Nervous System Is Associated with Oxidative Damage to Neurons. Virology **278:**309-321.

50. **van Lint, A., M. Ayers, A. G. Brooks, R. M. Coles, W. R. Heath, and F. R. Carbone.** 2004. Herpes Simplex Virus-Specific CD8+ T Cells Can Clear Established Lytic Infections from Skin and Nerves and Can Partially Limit the Early Spread of Virus after Cutaneous Inoculation. J Immunol **172:**392-397.

51. **Van Rooijen, N., and A. Sanders.** 1994. Liposome mediated depletion of macrophages: mechanism of action, preparation of liposomes and applications. J Immunol Methods **174:**83-93.

52. **Wang, J., and I. L. Campbell.** 2005. Innate STAT1-Dependent Genomic Response of Neurons to the Antiviral Cytokine Alpha Interferon. J. Virol. **79:**8295-8302.

53. **Waskow, C., S. Paul, C. Haller, M. Gassmann, and H. Rodewald.** 2002. Viable c-Kit(W/W) mutants reveal pivotal role for c-kit in the maintenance of lymphopoiesis. Immunity **17:**277-88.

54. **Whitley, R. J.** 2002. Herpes simplex virus infection. **13:**6-11.

55. **Whitley, R. J., and J. W. Gnann.** 2002. Viral encephalitis: familiar infections and emerging pathogens. Lancet **359:**507-13.

56. **Whitley, R. J., D. W. Kimberlin, and B. Roizman.** 1998. Herpes simplex viruses. Clin Infect Dis **26:**541-53; quiz 554-5.

57. **Zhou, J., S. A. Stohlman, D. R. Hinton, and N. W. Marten.** 2003. Neutrophils Promote Mononuclear Cell Infiltration During Viral-Induced Encephalitis. J Immunol **170:**3331-3336.

# Figure Legends.

**Figure 1. Visualization of Brainstem Lesions by MRI and Histology rom HSV Infected 129 and B6 mice.** Panel **A,** coronal T2-weighted MR images at the level of the trigeminal nerve root in four 129 mice at day 6 PI (panel **A,** 3 consecutive MR sections with arrows indicating increased signal in trigeminal nuclei) and four B6 mice (panel **B**, corresponding to section 2 in panel **A** with rectangles outlining area of trigeminal nucleus, not showing increased signal) (representative of 2 experiments). Hematoxylin and eosin stained brain stem frozen sections from an infected 129 mouse at day 7 PI (panel **C**, with extensive inflammatory infiltrate composed of neutrophils (black arrow) and mononuclear cells (white arrow)) and B6 mouse (panel **D**, corresponding section with scant inflammatory cells). Brain stem immunohistochemical staining at day 7 PI of 129 mice: positive for perivascular F4/80$^+$ macrophages (panel **E**), Gr-1$^+$ neutrophils (panel **G**), CD4$^+$ T cells (panel **I**), CD8$^+$ T cells (panel **K**), and HSV antigen (panel M) with corresponding negative immunochemical staining in B6 mice (panels **F, H, L, M**) except for occasional perivascular T cell as shown in panel J. Bar shown in panel **G** is 75 microns.

**Figure 2. Accumulation and activation of immune cells over time in brainstem of susceptible and resistant mice.** Cells were isolated from infected brainstems of B6 and 129 mice on day 6 or day 12 PI and analyzed for surface marker expression. **A** shows macrophages (CD11b$^+$ F4/80$^+$ CD45$^{hi}$) and **B** microglia (F4/80$^{low}$ CD45$^{int}$). **C.** The bar graphs indicate the absolute cell numbers of MHCII negative (open bars) and positive (filled bars) macrophages recovered from pooled brainstems (n=3). Mean fluorescence intensity (MFI) is indicated for the

MHCII$^+$ gates. Bar graphs of total MHCII density on macrophages (MP, white bars), microglia (MG, grey) and MP+MG (Total, black) in the BS of B6 (left) and 129 (right) mice on days 6 and 12 are shown. The MHCII density is calculated by multiplying the absolute number of MHCII+ cells by their MFI as indicated in **A** and **B** and provides a measure of relative amount of MHC molecules in the BS. **D.** MHCII expression on MG in three different CNS compartments of B6 (grey filled histograms) and 129 (open, thick line) mice on day 12. The MFI is also indicated for each strain. MG were gated as viable FSC-SSC, SSC-vs-CD45$^{int}$ events and data represent typical population profiles from pooled tissues of 2-4 mice and is representative of two experiments. The MHCII$^+$ gate is shown for each histogram overlay and the percentage positive cells for each strain and tissue is listed below each panel. **E.** Absolute numbers of CD4$^+$ CD45$^{hi}$ (left panel) or CD8$^+$ CD45$^{hi}$ (right panel) T-cells in BS from B6 and 129 mice on days 6 (open bars) and 12 (filled bars).

**Figure 3. Infiltrating Cells in the Brainstem of HSV Infected 129 Mice and Activation of Microglia.**

Cells isolated from brainstems of HSV-infected 129 mice at 38h and 62h PI stained for CD45 (**A**), and CD4 and CD8 (**B**) surface markers and activation molecules (MHCII or CD86 (**A**) and CD62L or CD69 (**B**), respectively). Increase in numbers and activation (loss of CD62L) of CD4 and CD8 T cells in draining lymph nodes on day 7 (**C**); not seen for CD4 and CD8 T cells retrieved from brainstems of the same mice (**D**). Brain stem cells stained for CD45 and MHCII show a continued increase in activation of microglia (CD45$^{int}$) until day 9 PI (peaks at 11.5% of total). (**E**). Absolute increases in macrophages (MP) and microglia (MG) relative to naïve mice

(Day 0) are indicated below the figure for days 4-9 PI. Representative of 3 experiments for **A** and **B** and 2 experiments for **C, D and E**.

**Figure 4. Depletion of Neutrophils or Macrophages during acute HSV infection Enhances Survival.**

Compared to MOCK treated 129 mice (open circles, dashed line; PBS or rat IgG), Gr-1 mAb (black squares), clodronate (grey squares) and combination treatment of both Gr-1 mAb and clodronate (black circles) significantly delayed mortality (mean survival prolonged to d12-13 versus d8 for controls). Survival on d10 was highly significant for all treatment groups ($p<0.003$ for each pairwise comparison to 129 MOCK controls). Data shown are combined from 5 different experiments. Overall statistical differences and the end of the experiments were as indicated: ** $p<0.005$, * $p<0.05$ relative to the MOCK group. ns = not significantly different.

**Figure 5. Transfer of susceptibility and resistance to Fatal HSE by BMT.**

**A.** B6-E mice were non-transplanted (red circles), given B6 BM (black squares), γ-irradiated and given 129 BM (blue down triangle) or non-irradiated and given 129 BM (green up triangle). Data for 129S6 mice are indicated for comparison (grey diamonds). As indicated by the arrow, four days after the last γ-irradiated 129-BMT mouse died, >80% of non-BMT mice were still alive (significant at $p=0.026$). Mice were infected by corneal scarification with 3200 PFU HSV-1 17+ and mortality monitored. Data combined from 4 experiments.

**B.** Duration of shedding in individual mice from the different groups (as indicated in the figure) is plotted with mean time of last day of shedding indicated (horizontal line). Horizontal bars above the graph indicate statistically significant differences between connected groups

(representative of two experiments). Brain stems from all four groups of BMT recipients in **A.** were examined for pathology associated with HSV infection. Occasional, or no, viral inclusions were found in neurons in non-transplanted controls and B6 BMT recipients (not shown). Abnormalities found in non-irradiated 129-BMT recipients were less severe than their γ-irradiated counterparts. Shown are sections from γ-irradiated 129-BMT mice. Cellular infiltrates are present in the subarachnoid space (**C**), perivascular parenchymal infiltrates in the brainstem (**D**) (neutrophils are shown in the inset), subpial infiltrating inflammatory cells (**E**), and prominent viral inclusions in the trigeminal nucleus (**F**). Inset shows higher magnification of several neurons with nuclear inclusions.

**Figure 6. Effect of Acyclovir (ACV) on Nervous System HSV Titer, Mortality, and Brain Stem Inflammation.**

129 mice were inoculated with HSV by corneal scarification and given daily intraperitoneal injections with PBS (grey symbols) or 50 mg/kg ACV (black symbols) from day 4 - 10 PI. **A**. HSV titers of trigeminal ganglia (squares) and brainstem (circles) (data from 1 of 2 trials with 2 mice in each group sacrificed at days 6and 8 PI); **B**. mortality due to HSE (n=20 control, n=14 ACV); **C**. brainstem infiltrating mononuclear cells at day 10 PI ($CD45^{high}$ cells are peripheral leukocytes while $CD45^{int}$ cells are $CD11b^{+}$ microglia).

**Table 1: Mouse Strain Differences in TLR expression**

| Gene | B6 $\Delta C_t$[a] | 129 $\Delta C_t$ | Difference $(2^{\Delta\Delta t})$[b] |
|---|---|---|---|
| muTLR2 | 8.7 | 8.4 | No difference |
| muTLR3 | ND | ND | ND |
| muTLR4 | 4.8 | 4.4 | No difference |
| muTLR6 | 32.9 | 24.0 | 129 is 480 X higher |
| muTLR7 | 12.3 | 12.6 | No difference |
| muTLR9 | 3.6 | 2.5 | 129 is 2.2 X higher |

cDNA from PEC-derived RNA from naive wild-type mice was used as template for SYBR green PCR amplification using primers for the target indicated in the column marked "Gene". Data combined from 4 experiments.
a; $DC_t$ is calculated as net Ct difference relative to GAPDH
b; $2^{DDt}$ is calculated as the $DC_t$ difference between B6 and 129,
ND; not done

| Group | Date | ID | d1 | d2 | d3 | d4 | d5 | d6 | d7 | d8 | d9 | d10 | d11 | d12 | d13 | d14 |
|---|---|---|---|---|---|---|---|---|---|---|---|---|---|---|---|---|
| B6-BMT | | A-1 | + | + | + | + | - | - | + | + | - | - | - | - | - | - |
| | | A-2 | + | + | ++ | + | + | - | + | - | - | - | - | - | - | - |
| | | A-3 | + | + | + | + | - | + | - | - | - | - | - | - | - | - |
| | | A-4 | + | + | + | + | + | + | - | - | - | - | - | - | - | - |
| | | A-5 | + | + | ++ | + | + | + | - | - | - | - | - | - | - | - |
| | | A-6 | + | + | + | - | + | + | + | - | - | - | - | - | - | - |
| | | A-7 | + | + | + | - | - | - | + | - | - | - | - | - | - | - |
| | | A-8 | + | + | ++ | + | + | + | ++ | + | - | - | - | - | - | - |
| | | A-9 | + | + | + | + | - | + | - | - | - | - | - | - | - | - |
| | | A-10 | + | + | ++ | + | - | + | - | - | - | - | - | - | - | - |
| | | A-11 | + | + | ++ | + | + | + | ++ | + | - | - | - | - | - | - |
| noBMT | d20 | B-12 | - | + | ++ | + | + | + | + | + | + | + | + | + | + | + |
| | d24 | B-13 | - | + | +++ | + | + | + | + | + | ++ | +++ | ++ | ++ | +++ | + |
| | d77 | B-14 | + | + | ++ | + | - | + | + | - | - | - | - | - | - | - |
| | | B-15 | - | + | +++ | + | - | - | ++ | ++ | ++ | + | + | ++ | +++ | +++ |
| | | B-16 | + | + | +++ | + | + | + | + | - | - | + | ++ | + | + | + |
| 129-BMT | | C-17 | + | + | + | + | - | - | - | + | - | - | - | - | - | - |
| | | C-18 | + | + | + | + | + | + | - | + | - | - | - | - | - | - |
| | | C-19 | + | + | ++ | + | + | - | + | - | + | - | - | - | - | - |
| | | C-20 | + | + | ++ | + | + | - | + | + | - | - | - | - | - | - |
| | | C-21 | + | + | + | + | + | - | - | + | + | - | - | - | - | - |
| | | C-22 | + | + | + | + | + | - | - | - | - | - | - | - | - | - |
| | | C-23 | + | + | + | + | + | - | - | + | - | - | - | - | - | - |
| | d11 | C-24 | + | + | + | + | + | + | ++ | + | - | - | - | - | - | - |
| γ129-BMT | | D-25 | + | + | + | + | + | + | - | + | - | - | - | - | - | - |
| | d11 | D-26 | + | + | + | + | + | + | + | + | - | + | - | - | - | - |
| | | D-27 | + | + | + | - | - | - | - | - | - | - | - | - | - | - |
| | d17 | D-28 | + | + | + | + | - | + | + | + | - | - | - | - | - | - |
| | | D-29 | + | + | + | - | - | - | + | - | - | - | - | - | - | - |
| | | D-30 | - | + | + | + | - | - | - | - | - | - | - | - | - | - |
| | d13 | D-31 | - | + | + | + | - | + | ++ | - | - | - | - | - | - | - |
| | | D-32 | + | + | + | - | - | + | ++ | - | - | - | - | - | - | - |
| | d13 | D-33 | + | + | ++ | - | + | + | ++ | - | + | - | - | - | - | - |

**Table 2. HSV shedding in tear film from BMT mice during acute infection.** 'Group' indicates donor BM source (γ=recipient was irradiated before BMT). Mice that died are indicated under 'Date' to the left of mouse 'ID'. All mice were swabbed daily until d14, and the 3 mice surviving in the noBMT group were additionally swabbed on days 24 and 39 and determined to be free of virus in the tear film (not shown). The amount of virus in tear film is indicated for no virus detected (-), <10 plaques in swab (+), 10-50 plaques (++), and >50 plaques (+++). Data from one of two representative experiments.

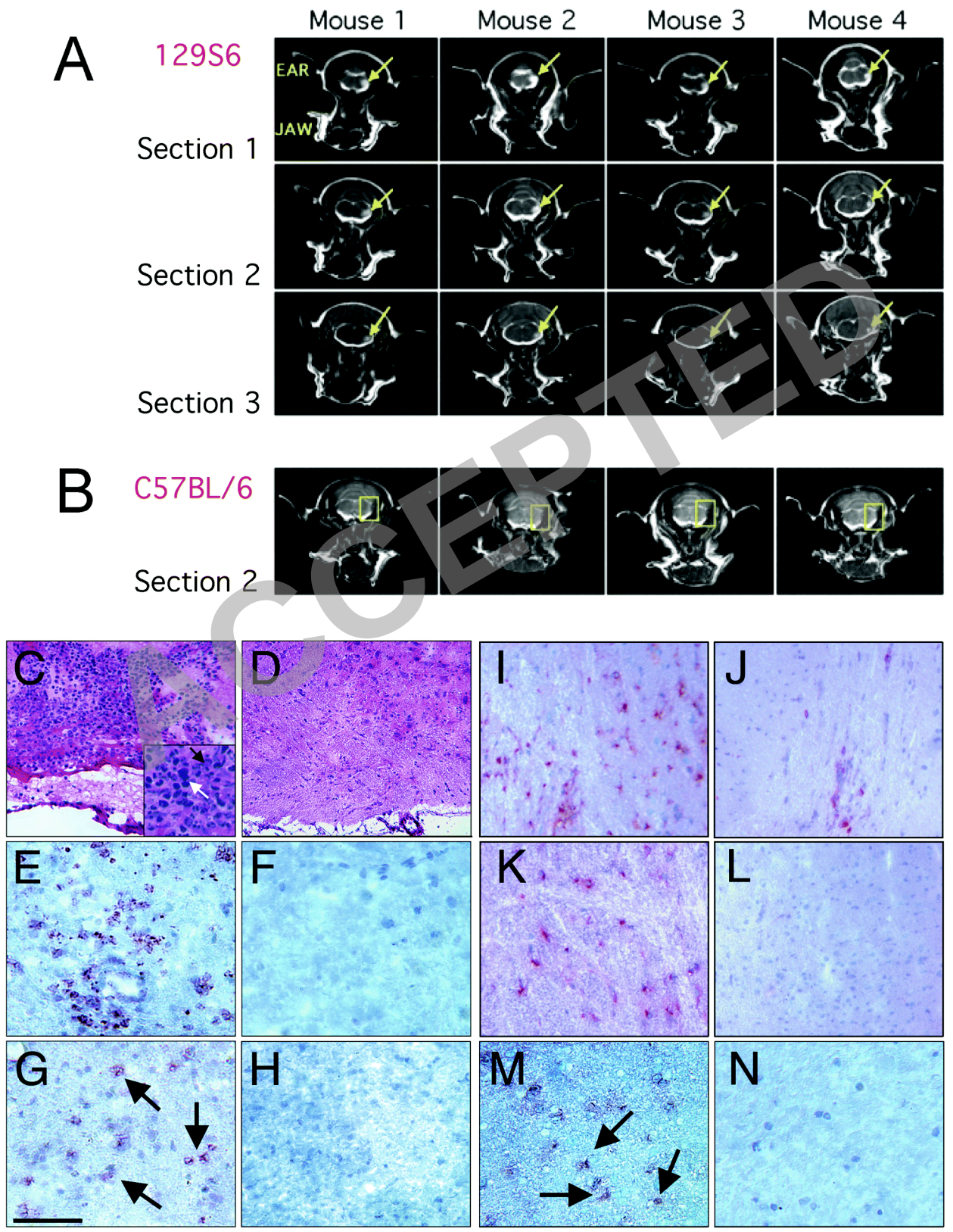
Mouse 1
Mouse 2
Mouse 3
Mouse 4
A
129S6
EAR
JAW
Section 1
Section 2
Section 3
B
C57BL/6
Section 2
C
D
I
J
E
F
K
L
G
H
M
N

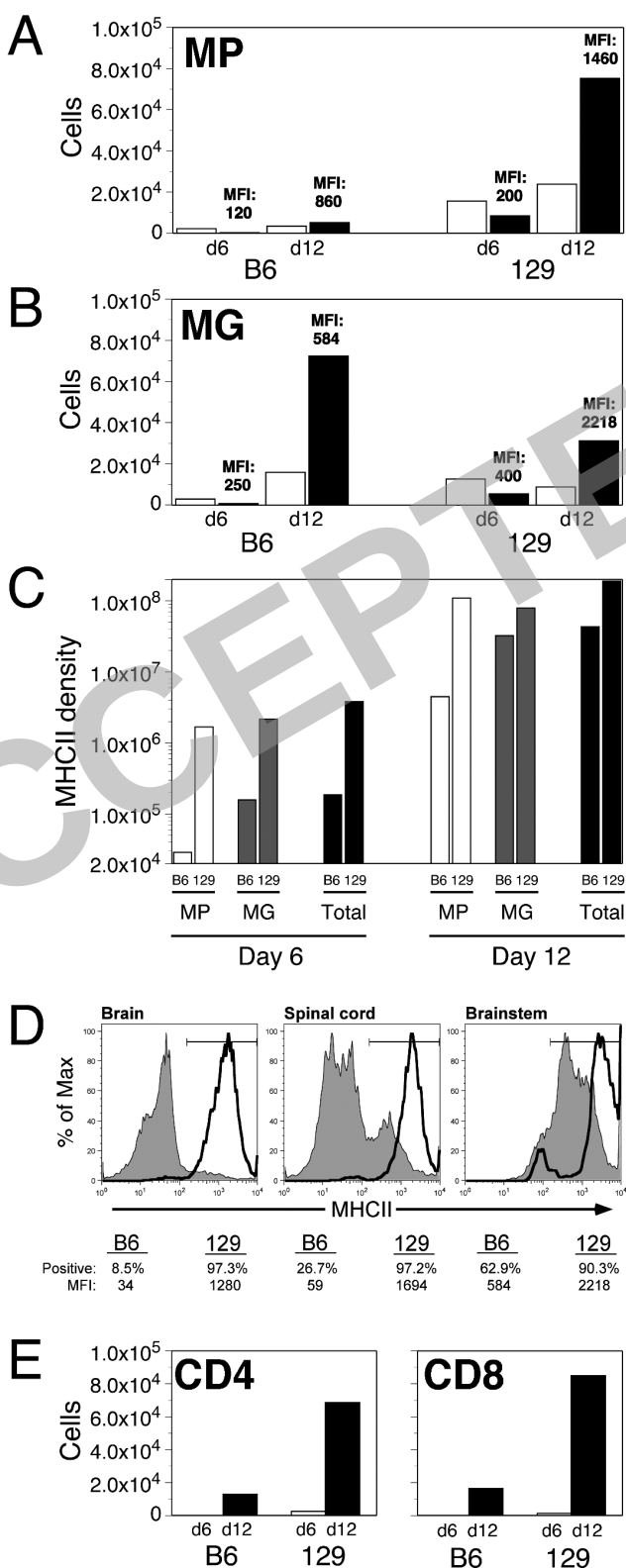
A
MP
Cells
1.0x10^5
8.0x10^4
6.0x10^4
4.0x10^4
2.0x10^4
0
MFI: 120
MFI: 860
MFI: 200
MFI: 1460
d6
d12
B6
129
B
MG
MFI: 584
MFI: 250
MFI: 2218
MFI: 400
C
MHCII density
1.0x10^8
1.0x10^7
1.0x10^6
1.0x10^5
2.0x10^4
B6 129
MP
MG
Total
Day 6
Day 12
D
Brain
Spinal cord
Brainstem
% of Max
MHCII
B6
129
Positive: 8.5% 97.3% 26.7% 97.2% 62.9% 90.3%
MFI: 34 1280 59 1694 584 2218
E
CD4
CD8

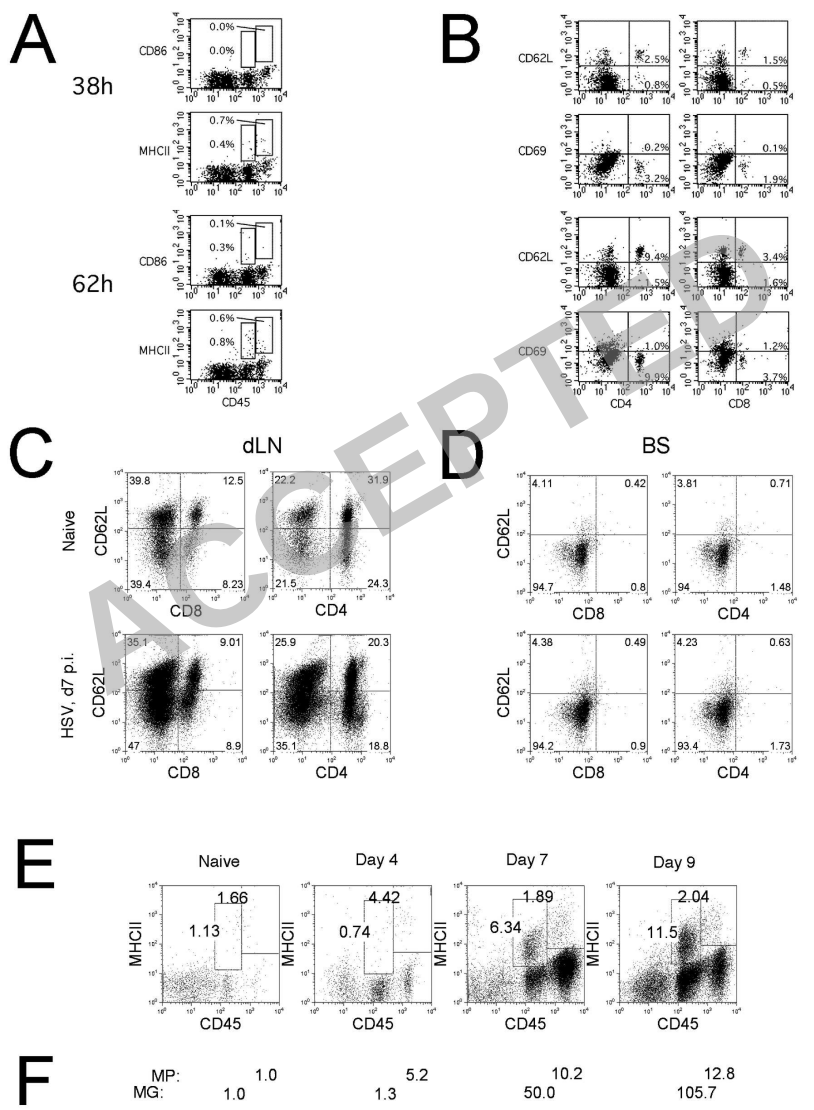
A
38h
CD86
0.0%
0.0%
MHCII
0.7%
0.4%
62h
CD86
0.1%
0.3%
MHCII
0.6%
0.8%
CD45
B
CD62L
2.5%
0.8%
1.5%
0.5%
CD69
0.2%
3.2%
0.1%
1.9%
CD62L
9.4%
3.4%
CD69
1.0%
0.9%
1.2%
3.7%
CD4
CD8
C
dLN
Naive
CD62L
39.8
12.5
39.4
8.23
22.2
31.9
21.5
24.3
CD8
CD4
HSV, d7 p.i.
CD62L
35.1
9.01
47
8.9
25.9
20.3
35.1
18.8
CD8
CD4
D
BS
CD62L
4.11
0.42
94.7
0.8
3.81
0.71
94
1.48
CD8
CD4
CD62L
4.38
0.49
94.2
0.9
4.23
0.63
93.4
1.73
CD8
CD4
E
Naive
Day 4
Day 7
Day 9
MHCII
1.66
1.13
4.42
0.74
1.89
6.34
2.04
11.5
CD45
F
MP:
MG:
1.0
1.0
5.2
1.3
10.2
50.0
12.8
105.7

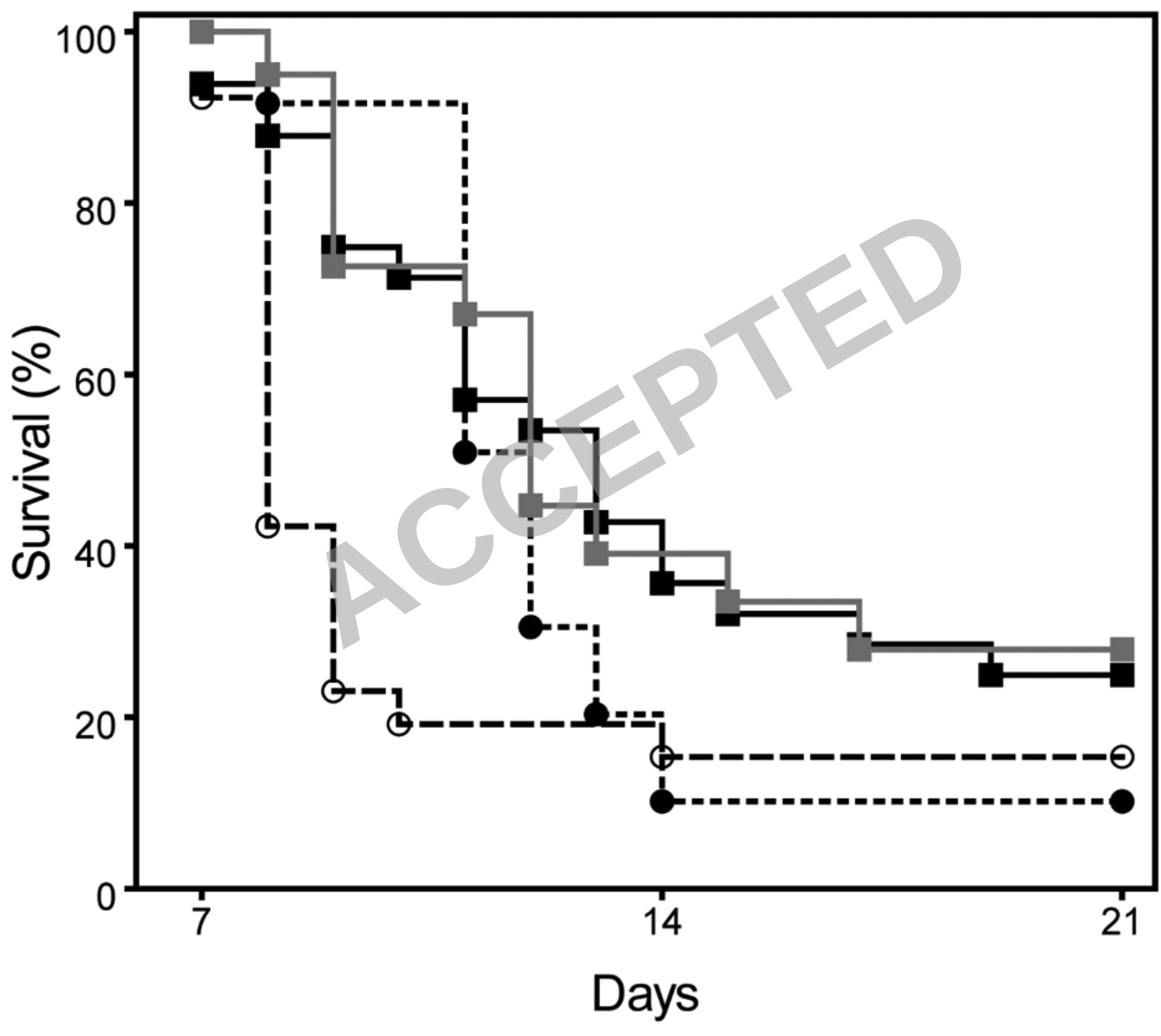

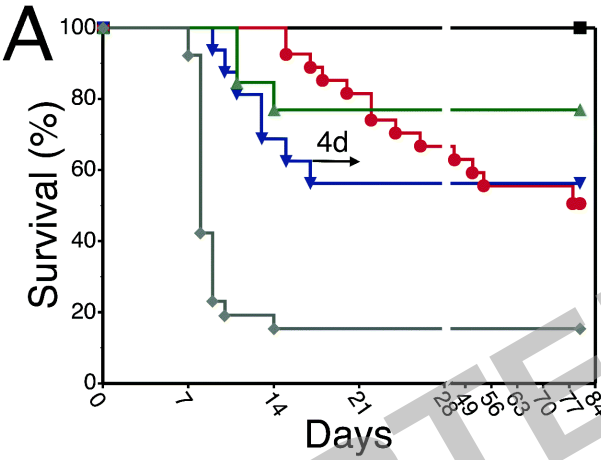
A
Survival (%)
100
80
60
40
20
0
4d
0
7
14
21
28
49
56
63
70
77
84
Days

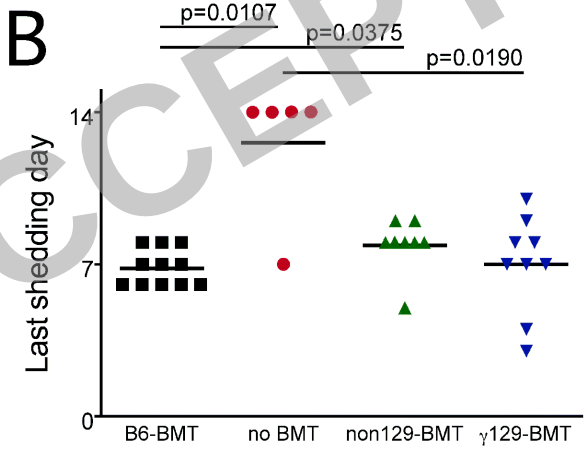
B
p=0.0107
p=0.0375
p=0.0190
Last shedding day
14
7
0
B6-BMT
no BMT
non129-BMT
γ129-BMT

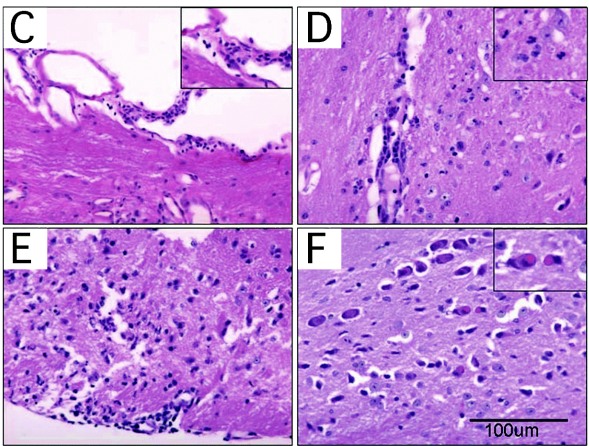
C
D
E
F
100um

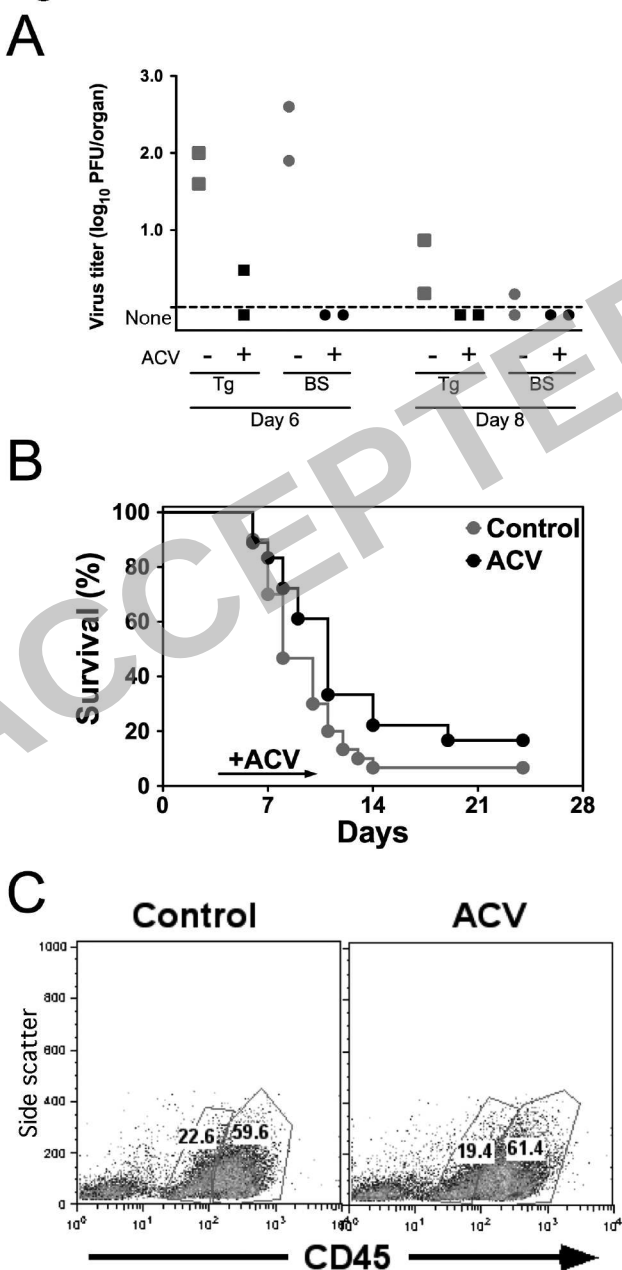
A
Virus titer ($log_{10}$ PFU/organ)
3.0
2.0
1.0
None
ACV - + - + - + - +
Tg BS Tg BS
Day 6 Day 8
B
Survival (%)
100
80
60
40
20
0
Control
ACV
+ACV
0 7 14 21 28
Days
C
Control
ACV
Side scatter
22.6 59.6
19.4 61.4
CD45